JACS
ARTICLES

A Reduced β-Diketiminato-Ligated Ni_3H_4 Unit Catalyzing H/D Exchange

Stefan Pfirrmann,[†] Christian Limberg,*[,†] Christian Herwig,[†] Christina Knispel,[†]
Beatrice Braun,[†,‡] Eckhard Bill,[§] and Reinhard Stösser[†]

*Humboldt-Universität zu Berlin, Institut für Chemie, Brook-Taylor-Strasse 2,
12489 Berlin, Germany, RWTH Aachen University, Institute of Inorganic Chemistry, Landoltweg
1, 52074 Aachen, Germany, Max-Planck-Institut für Bioanorganische Chemie, Stiftstrasse 34-36,
45470 Mülheim/Ruhr, Germany*

Received March 26, 2010; E-mail: christian.limberg@chemie.hu-berlin.de

Abstract: An investigation concerning the stepwise reduction of the β-diketiminato nickel(II) hydride dimer $[LNi(\mu\text{-}H)_2NiL]$, **1** ($L = [HC(CMeNC_6H_3(i\text{Pr})_2)_2]^-$), has been carried out. While the reaction with one equivalent of potassium graphite, KC_8, led to the mixed valent Ni^I/Ni^{II} complex $K[LNi(\mu\text{-}H)_2NiL]$, **3**, treatment of **1** with two equivalents of KC_8 surprisingly yielded in the trinuclear complex $K_2[LNi(\mu\text{-}H)_2Ni(\mu\text{-}H)_2NiL]$, **4**, in good yields. The Ni_3H_4 core contains one Ni^{II} and two Ni^I centers, which are antiferromagnetically coupled so that a singlet ground state results. **4** represents the first structurally characterized molecular compound with three nickel atoms bridged by hydride ligands, and it shows a very interesting chemical behavior: Single-electron oxidation yields in the $Ni^{II}{}_2Ni^I$ compound $K[LNi(\mu\text{-}H)_2Ni(\mu\text{-}H)_2NiL]$, **5**, and treatment with CO leads to the elimination of H_2 with formation of the carbonyl complex $K_2[LNi(CO)]_2$, **6**. Beyond that, it could be shown that **4** undergoes H/D exchange with deuterated solvents and the deuteride-compound **4-D$_4$** reacts with H_2 to give back **4**. The crystal structures of the novel compounds **3**−**6** have been determined, and their electronic structures have been investigated by EPR and NMR spectroscopy, magnetic measurements, and DFT calculations.

Introduction

Nickel hydride units play decisive roles in many catalytic processes applied in industrial or academic laboratories,[1] and this already accounts for a high interest in Ni−H coordination compounds.[2−6] The intriguing function of [NiFe]-hydrogenases provides further motivation for corresponding investigations. Their prosthetic groups contain a nickel center coordinated by two cysteinate ligands as well as an iron center, which binds two cyanide and one CO ligand, and these two units are bridged by two additional cysteinate ligands.[7] [NiFe]-hydrogenases catalyze the reversible two-electron oxidation of dihydrogen to protons as part of their energy metabolism (with a preference for H_2 consumption) and thereby allow the generation or disposal of reducing equivalents.[8] The mechanism, by which this very simple redox reaction is accomplished, is still a matter of intense research and debate. Biochemical investigations revealed several redox and protonation states of the enzyme, including several different EPR active states.[9] On the basis of the results emerging from structural data, advanced EPR spectroscopic studies, and density functional calculations the central intermediate within the catalytic cycle of the [NiFe]-hydrogenase active site is proposed to contain a bridging hydride ligand between the Ni and the Fe centers.[10] Considering that according to all spectroscopic studies the nickel portion is the major component of the active site, where all of the redox chemistry takes place, the background outlined above provides

---

[†] Humboldt-Universität zu Berlin.

[‡] RWTH Aachen University.

[§] Max-Planck-Institut für Bioanorganische Chemie.

(1) (a) Kokes, R. J.; Emmett, P. H. *J. Am. Chem. Soc.* **1959**, *81*, 5032–5037. (b) Keim, W.; Behr, A.; Limbäcker, B.; Krüger, C. *Angew. Chem., Int. Ed.* **1983**, *22*, 503. (c) Keim, W.; Appel, R.; Gruppe, S.; Knoch, F. *Angew. Chem., Int. Ed.* **1987**, *26*, 1012–1013. (d) *Recent advances in hydride chemistry*, 1st ed.; Peruzzini, M.; Poli, R., Eds.; Elsevier: Amsterdam, 2001. (e) Kogut, E.; Zeller, A.; Warren, T. H.; Strassner, T. *J. Am. Chem. Soc.* **2004**, *126*, 11984–11994.

(2) (a) Clement, N. D.; Cavell, K. J.; Jones, C.; Elsevier, C. J. *Angew. Chem., Int. Ed.* **2004**, *43*, 1277–1279. (b) Yang, J. Y.; Bullock, R. M.; Shaw, W. J.; Twamley, B.; Fraze, K.; DuBois, M. R.; DuBois, D. L. *J. Am. Chem. Soc.* **2009**, *131*, 5935–5945. (c) Chakraborty, S.; Krause, J. A.; Guan, H. *Organometallics* **2009**, *28*, 582–586. (d) Tran, B. L.; Pink, M.; Mindiola, D. J. *Organometallics* **2009**, *28*, 2234–2243.

(3) Steinke, T.; Gemel, C.; Cokoja, M.; Winter, M.; Fischer, R. A. *Angew. Chem., Int. Ed.* **2004**, *43*, 2299–2302.

(4) Chen, W.; Shimada, S.; Tanaka, M.; Kobayashi, Y.; Saigo, K. *J. Am. Chem. Soc.* **2004**, *126*, 8072–8073.

(5) Liang, L.-C.; Chien, P.-S.; Lee, P.-Y. *Organometallics* **2008**, *27*, 3082–3093.

(6) Laird, M. F.; Pink, M.; Tsvetkov, N. P.; Fan, H.; Caulton, K. G. *Dalton Trans.* **2009**, 1283–1285.

(7) (a) Volbeda, A.; Garcin, E.; Piras, C.; de Lacey, A. L.; Fernandez, V. M.; Hatchikian, E. C.; Frey, M.; Fontecilla-Camps, J. C. *J. Am. Chem. Soc.* **1996**, *118*, 12989–12996. (b) Volbeda, A.; Charon, M.-H.; Piras, C.; Hatchikian, E. C.; Frey, M.; Fontecilla-Camps, J. C. *Nature* **1995**, *373*, 580–587.

(8) (a) Frey, M. *ChemBioChem* **2002**, *3*, 153–160. (b) Harrop, T. C.; Mascharak, P. K. in *Concepts and models in bioinorganic chemistry*; Kraatz, H.-B., Metzler-Nolte, N., Eds.; Wiley-VCH: Weinheim, 2006.

(9) (a) Surerus, K. K.; Chen, M.; van der Zwaan, J. W.; Rusnak, F. M.; Kolk, M.; Duin, E. C.; Albracht, S. P. J.; Muenck, E. *Biochemistry* **1994**, *33*, 4980–4993. (b) Roberts, L. M.; Lindahl, P. A. *J. Am. Chem. Soc.* **1995**, *117*, 2565–2572. (c) Bleijlevens, B.; van Broekhuizen, F. A.; de Lacey, A. L.; Roseboom, W.; Fernandez, V. M.; Albracht, S. P. J. *J. Biol. Inorg. Chem.* **2004**, *9*, 743–752.

10.1021/ja106266v

a strong impetus for fundamental studies on the redox chemistry of nickel complexes containing bridging hydride ligands. With this background we set out exploring nickel hydride chemistry in combination with bulky β-diketiminato ligand systems, which have proven very versatile in the past: They stabilize high as well as low oxidation states and can be applied to prepare complexes with low coordination numbers.[11] Recently, we have reported the successful synthesis of the compound $[LNi(\mu\text{-}H)_2NiL]$, **1** ($L = [HC(CMeNC_6H_3(iPr)_2)_2]^-$, see Scheme 1),[12] which proved to be very reactive. On addition of simple donors such as pyridines and nitriles, immediately H_2 is reductively eliminated with concomitant formation of LNi^I complexes, and even upon dissolution of **1** in toluene, warming leads to the dinuclear complex $[(LNi)_2(\mu\text{-}\eta^3{:}\eta^3\text{-}C_6H_5Me)]$, **2**.[13] On the other hand, in the absence of suitable donors, H_2 was shown to oxidatively add to certain LNi^I compounds generated from Ni^{II} precursors by treatment with KC_8.[14] In particular the latter finding is interesting in the context of a recent mechanistic proposal made for the functioning of the [NiFe]-hydrogenases active site being based on the oxidative addition of H_2 to a Ni^I intermediate.[15] We were thus interested in a further exploration of LNiH chemistry under reducing conditions, and a recent report concerning the first $L'Co^IH$ ($L' = [HC(C(CMe_3)NC_6H_3(iPr)_2)_2]^-$) compound represented further motivation.[16]

Experimental Section

General Considerations. All experiments were carried out in a dry nitrogen/argon atmosphere using a glovebox and/or standard Schlenk techniques. Solvents were purified employing an MBraun Solvent Purification System SPS. Deuterated solvents were purified using appropriate techniques. NMR spectra were recorded on a Bruker AV 400 NMR spectrometer (^{1}H 400.13 MHz; ^{2}H 61.42 MHz; ^{13}C 100.63 MHz). Chemical shifts are reported in ppm relative to residual proton signals and natural-abundance ^{13}C resonances of C_6D_6 at 7.15 ppm and 128.02 ppm, respectively. IR spectra were recorded on solid samples prepared as KBr pellets with a Shimadzu FTIR-8400S spectrometer. Microanalyses were performed on a HEKAtech Euro EA 3000 elemental analyzer. Compounds $[LNi(\mu\text{-}H)]_2$, **1**, ($L = [HC(CMeNC_6H_3(iPr)_2)_2]^-$),[12] LK,[17] and TlOTf[18] were prepared according to the literature methods. $[LNi(\mu\text{-}D)]_2$, **1-D$_2$**, was synthesized in close analogy to the reported synthesis of $[LNi(\mu\text{-}H)]_2$, **1**, using $LiBEt_3D$.

Synthesis of K[LNi(μ-H)]$_2$, 3. $[LNi(\mu\text{-}H)]_2$ (0.244 g, 0.26 mmol) and KC_8 (0.038 g, 0.28 mmol, 1.1 equiv) were suspended in 10 mL of hexane, and the reaction mixture was stirred for 16 h at room temperature, resulting in a color change from green to brown. After filtration and concentration of the filtrate to approximately 5 mL in vacuum, the solution was cooled to −30 °C for 2 days, affording dark-brown, needle-like crystals of $K[LNi(\mu\text{-}H)]_2\cdot 1/2\text{hexane}\cdot 1/2\text{heptane}$ (0.064 g, 0.06 mmol, 25%); elemental analysis (%) calc. for $C_{64.50}H_{99}KN_4Ni_2$ (1087.00 g mol^{-1}): C 71.27, H 9.18, N 5.15; found: C 69.81, H 8.94, N 5.26 (consistently low C analyses may result from formation of NiC upon combustion); IR (KBr): $\tilde{\nu}$ = 3051 (w), 2959 (vs), 2922 (s), 2864 (s), 1539 (s), 1515 (s), 1463 (s), 1431 (vs), 1402 (vs), 1366 (s), 1314 (s), 1258 (m), 1252 (m), 1224 (m), 1173 (s), 1104 (m), 1057 (w), 1017 (m), 929 (w), 848 (w), 794 (s), 761 (s), 735 (m), 715 (w).

Synthesis of K[LNi(μ-D)]$_2$, 3-D$_2$. The synthesis of **3-D$_2$** was achieved by the same procedure as reported above for **3** but employing **1-D$_2$**.

Synthesis of K$_2$[(LNi)$_2$Ni(μ-H)$_4$], 4. $[LNi(\mu\text{-}H)]_2$ (0.340 g, 0.36 mmol) and KC_8 (0.107 g, 0.79 mmol, 2.2 equiv) were suspended in 10 mL of hexane, and the reaction mixture was stirred for 16 h at room temperature, resulting in a color change from green to dark purple. After filtration and concentration to approximately 5 mL in vacuum, the solution was cooled to −30 °C for 2 days, affording black-purple crystals of $K_2[(LNi)_2Ni(\mu\text{-}H)_4]\cdot\text{hexane}$ (0.102 g, 0.09 mmol, 48% based on the reaction stoichiometry); elemental analysis (%) calc. for $C_{64}H_{100}K_2N_4Ni_3$ (1179.78 g mol^{-1}): C 65.15, H 8.54, N 4.75; found: C 63.99, H 8.41, N 4.78 (consistently low C analyses may result from formation of NiC upon combustion); ^{1}H NMR (400.13 MHz, C_6D_6, rt): δ = 6.75 (d, $^3J_{HH}$ = 7.5 Hz, 8H, Ar-*mH*), 6.19 (t, $^3J_{HH}$ = 7.5 Hz, 4H, Ar-*pH*), 4.73 (s, 2H, C*H*CCH$_3$), 4.44 (m, 8H, C*H*(CH$_3$)$_2$), 1.88 (d, $^3J_{HH}$ = 6.6 Hz, 24H, CH(C*H*$_3$)$_2$), 1.19 (d, $^3J_{HH}$ = 6.9 Hz, 24H, CH(C*H*$_3$)$_2$), 1.04 (s, 12H, NCC*H*$_3$), −38.40 ppm (s, br, 4H, Ni-*H*); ^{13}C{^{1}H} NMR (100.6 MHz, C_6D_6, rt): δ = 158.4 (N*C*CH$_3$), 150.3 (Ar-*iC*), 143.7 (Ar-*oC*), 123.5 (Ar-*pC*), 121.0 (Ar-*mC*), 98.6 (*C*HCCH$_3$), 27.2 (NC*C*H$_3$, *C*H(CH$_3$)$_2$), 26.2 (CH(*C*H$_3$)$_2$), 23.4 ppm (CH(*C*H$_3$)$_2$); IR (KBr): $\tilde{\nu}$ = 3047 (w), 3005 (w), 2955 (vs), 2922 (vs), 2914 (vs), 2867 (s), 2853 (s), 1577 (w), 1523 (vs), 1465 (vs), 1461 (vs), 1429 (vs), 1410 (vs), 1382 (s), 1366 (m), 1357 (m), 1323 (vs), 1263 (m), 1254 (m), 1243 (m), 1226 (s), 1179 (s), 1155 (m), 1095 (s), 1057 (m), 1040 (w), 1027 (m), 953 (vw), 934 (w), 922 (vw), 882 (w), 854 (w), 849 (w), 794 (vs), 763 (s), 733 (m), 714 (w).

Synthesis of K[(LNi)$_2$Ni(μ-H)$_4$], 5. $K_2[(LNi)_2Ni(\mu\text{-}H)_4]\cdot\text{hexane}$ (0.057 g, 0.05 mmol) and TlOTf (0.017 g, 0.05 mmol) were suspended in 10 mL of diethyl ether, and the reaction mixture was stirred for 16 h at room temperature, resulting in a color change from dark purple to green. Filtration of the suspension, concentration of the green filtrate to 5 mL, and cooling to −30 °C afforded dark-green crystals of $K[(LNi)_2Ni(\mu\text{-}H)_4]\cdot\text{diethyl ether}$ (0.030 g, 0.03 mmol, 54%); elemental analysis (%) calc. for $C_{62}H_{96}KN_4Ni_3O$ (1128.63 g mol^{-1}): C 65.98, H 8.57, N 4.96; found: C 64.66, H 8.03, N 5.06 (consistently low C analyses may result from formation of NiC upon combustion); IR (KBr): $\tilde{\nu}$ = 3054 (w), 2959 (vs), 2923 (s), 2865 (m), 1542 (s), 1525 (vs), 1462 (s), 1434 (vs), 1400 (vs), 1359 (m), 1320 (vs), 1258 (m), 1253 (m), 1230 (m), 1182 (m), 1098 (m), 1057 (m), 1028 (m), 934 (w), 858 (w), 804 (m), 796 (m), 758 (s).

Synthesis of K[(LNi)$_2$Ni(μ-D)$_4$], 5-D$_4$. A solution of $K_2[(LNi)_2Ni(\mu\text{-}H)_4]$, **4**, in toluene-$d_8$ was heated to 60 °C until the hydride signal at −38 ppm had disappeared in the ^{1}H NMR spectrum of samples taken. Subsequently, 1 equiv of TlOTf was added, and the reaction mixture was stirred for 16 h, resulting in a color change from dark purple to green. After filtration of the suspension the green solution obtained was used for the EPR experiments.

Synthesis of K$_2$[LNi(CO)]$_2$, 6. A solution of $K_2[(LNi)_2Ni(\mu\text{-}H)_4]\cdot\text{hexane}$ (0.043 g, 0.04 mmol) in 10 mL of hexane was exposed to an atmosphere of carbon monoxide, causing an immediate color change from dark purple to orange brown. The reaction mixture was stirred for 10 min and reduced to 3 mL in vacuum. Cooling and evaporation of the solution at −30 °C afforded orange crystals of $K_2[LNi(CO)]_2\cdot\text{hexane}$ (0.021 g, 0.018 mmol,

---

(10) (a) Brecht, M.; van Gastel, M.; Buhrke, T.; Friedrich, B.; Lubitz, W. *J. Am. Chem. Soc.* **2003**, *125*, 13075–13083. (b) Foerster, S.; Stein, M.; Brecht, M.; Ogata, H.; Higuchi, Y.; Lubitz, W. *J. Am. Chem. Soc.* **2003**, *125*, 83–93. (c) Mealli, C.; Rauchfuss, T. B. *Angew. Chem., Int. Ed.* **2007**, *46*, 8942–8944. (d) Barton, B. E.; Whaley, C. M.; Rauchfuss, T. B.; Gray, D. L. *J. Am. Chem. Soc.* **2009**, *131*, 6942–6943.

(11) (a) Bourget-Merle, L.; Lappert, M. F.; Severn, J. R. *Chem. Rev.* **2002**, *102*, 3031–3066. (b) Mindiola, D. J. *Angew. Chem., Int. Ed.* **2009**, *48*, 6198–6200.

(12) Pfirrmann, S.; Limberg, C.; Ziemer, B. *Dalton Trans.* **2008**, 6689–6691.

(13) Bai, G.; Wei, P.; Stephan, D. W. *Organometallics* **2005**, *24*, 5901–5908.

(14) Pfirrmann, S.; Yao, S.; Ziemer, B.; Stösser, R.; Driess, M.; Limberg, C. *Organometallics* **2009**, *28*, 6855–6860.

(15) Nilsson Lill, S. O.; Siegbahn, P. E. M. *Biochemistry* **2009**, *48*, 1056–1066.

(16) Ding, K.; Brennessel, W. W.; Holland, P. L. *J. Am. Chem. Soc.* **2009**, *131*, 10804–10805.

(17) Chai, J.; Zhu, H.; Most, K.; Roesky, H. W.; Vidovic, D.; Schmidt, H.-G.; Noltemeyer, M. *Eur. J. Inorg. Chem.* **2003**, 4332–4337.

(18) Fox, B. J.; Millard, M. D.; DiPasquale, A. G.; Rheingold, A. L.; Figueroa, J. S. *Angew. Chem., Int. Ed.* **2009**, *48*, 3473–3477.

45%); elemental analysis (%) calc. for $C_{66}H_{96}K_2N_4Ni_2O_2$ (1173.50 g mol^{-1}): C 67.57, H 8.25, N 4.78; found: C 65.90, H 8.40, N 4.79 (consistently low C analyses may result from formation of NiC upon combustion); ^{1}H NMR (400.13 MHz, C_6D_6, rt): $\delta = 7.04$ (m, 8H, Ar-*mH*), 6.92 (m, 4H, Ar-*pH*), 4.81 (s, 2H, C*H*CCH$_3$), 3.78 (m, 8H, C*H*(CH$_3$)$_2$), 1.69 (s, 12H, NCC*H*$_3$), 1.48 (d, $^3J_{HH} =$ 5.5 Hz, 24H, CH(C*H*$_3$)$_2$), 1.22 ppm (m, 24H, CH(C*H*$_3$)$_2$); $^{13}C\{^1H\}$ NMR (100.6 MHz, C_6D_6, rt): $\delta = 200.9$ (*C*O) 158.0 (N*C*CH$_3$), 152.9 (Ar-*iC*), 140.9 (Ar-*oC*), 123.3 (Ar-*mC*), 123.1 (Ar-*pC*), 94.9 (*C*HCCH$_3$), 28.0 (*C*H(CH$_3$)$_2$), 24.1 (CH(*C*H$_3$)$_2$), 23.5 (CH(*C*H$_3$)$_2$), 22.9 ppm (NC*C*H$_3$); IR (KBr): $\tilde{\nu} = 3056$ (w), 2958 (s), 2921 (m), 2866 (m), 1772, 1754 (vs, ν_{CO}, 1727, 1711 for ^{13}CO), 1525 (s), 1463 (s), 1433 (vs), 1404 (vs), 1368 (m), 1359 (m), 1323 (s), 1256 (m), 1228 (m), 1181 (m), 1100 (m), 1058 (w), 1023 (w), 934 (w), 797 (m), 764 (m), 743 (m).

Crystal Structure Determinations. Data collections were performed at 100 K with a Bruker Smart APEX CCD area detector on a D8 goniometer for **3** and **6** and on a Stoe IPDS 2T diffractometer for **4** and **5**. Mo-K_α radiation ($\lambda = 0.71073$ Å) was used for all experiments; radiation source was an INCOATEC microsource with multilayer optics for **3** and **6** and a sealed-tube generator with graphite monochromator for **4** and **5**. SADABS[19] absorption correction was applied for **3** and **6**, a numerical absorption correction, for **4**, and multiscan (PLATON)[20] absorption correction, for **5**. The structures were solved by direct methods (SHELXS-97)[21] and refined by full matrix least-squares procedures based on F^2 with all measured reflections (SHELXL-97).[22] All non-hydrogen atoms were refined anisotropically. H atoms were introduced in their idealized positions and refined as riding except for the bridging H atoms in **3**, **4**, and **5**. After completion of the structure models for **3**, **4**, and **5** with respect to the non-H atoms, a difference Fourier electron density map showed maxima in the upper part of the remaining peaks and in the geometry expected for a bridging hydride. After assignment of these positions as hydrogen atoms, the refinement of the positional coordinates and individual isotropic displacement parameters converged. The crystal structure of **3** is a racemic twin; instead of performing a Flack parameter refinement, the twin refinement was done.

Magnetic Susceptibility Measurements. Magnetic susceptibility data for **3** and **5** were measured from powder samples of solid material in the temperature range 2−300 K with a SQUID susceptometer with a field of 1.0 T (MPMS-7, Quantum Design, calibrated with standard palladium reference sample, error <1%). The experimental data were corrected for underlying diamagnetism by use of tabulated Pascal's constants,[23] as well as for temperature-independent paramagnetism (TIP). The susceptibility and magnetization data were simulated with our own package julX for exchange coupled systems.[24] The simulations are based on the usual spin-Hamilton operator for $S = 1/2$:

$$\hat{H} = g_{\mathrm{av}}\mu_{\mathrm{B}}\vec{S}\cdot\vec{B}$$

EPR Measurements. The X-band EPR derivative spectrum of **3** was recorded on a Bruker ELEXSYS E500 spectrometer equipped with the Bruker standard cavity (ER4102ST) and a helium flow cryostat (Oxford Instruments ESR 910). Microwave frequencies were calibrated with a Hewlett-Packard frequency counter (HP5352B), and the field control was calibrated with an S2 Bruker NMR field probe (ER035M). The spectrum was simulated with the program GFIT (by E. B.) for the calculation of powder spectra with effective *g* values and anisotropic line widths (Gaussian line shapes were used). EPR spectra of **5** were recorded at the X-band spectrometer ERS 300 (ZWG/Magnettech Berlin/Adlershof, Germany) equipped with a fused quartz Dewar for measurements at liquid nitrogen temperature. The *g* factors were calculated with respect to a Cr^{3+}/MgO reference ($g = 1.9796$). The spectra were simulated with the WINEPR simfonia package from Bruker for the calculation of powder spectra with effective *g* values and anisotropic line widths (Gaussian line shapes were used).

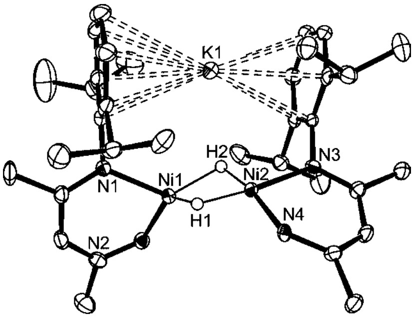

Figure 1. Molecular structure of **3** using 50% thermal ellipsoids. Solvent molecules, noncoordinating ligand aryl units and carbon−hydrogen atoms are omitted for clarity. Selected bond lengths (Å) and angles (°): Ni1−H1 1.61(5), Ni1−H2 1.64(5), Ni2−H1 1.49(5), Ni2−H2 1.43(5), Ni1−Ni2 2.4864(8), Ni1−N1 1.963(4), Ni1−N2 1.954(4), Ni2−N3 1.925(4), Ni2−N4 1.928(4), C13−N1 1.329(6), C16−N2 1.347(6), C42−N3 1.339(6), C45−N4 1.348(6); N1−Ni1−H1 104.0(19), N1−Ni1−H2 125(2), N2−Ni1−H1 132.5(19), N2−Ni1−H2 135.9(19), N3−Ni2−H1 168(2), N3−Ni2−H2 94(2), N4−Ni2−H1 97(2), N4−Ni2−H2 169(2).

Electronic Structure Calculations. Restricted and unrestricted density functional theory (DFT) calculations were carried out using the Gaussian 03 program package.[25] Geometry optimizations employing the B3LYP functional[26] together with the 6-31G** basis set[27] were performed for several spin states of **3**, utilizing the X-ray coordinates as initial input. The search for broken symmetry states was assisted by the program ORCA[28] (see Supporting Information for details). The program NBO 3.1[29] as implemented in Gaussian 03 was used for subsequent Natural Bond Orbital (NBO) analyses.

Results and Discussion

Treatment of **1** dissolved in hexane with one equivalent of KC_8 afforded a brown solution, from which brown crystals were obtained by cooling to −30 °C. The result of an X-ray diffraction analysis (see Figure 1) hinted to the successful single-electron reduction of the Ni_2H_2 core: As in the molecular structure of **1**, two hydride ligands could be located in the Fourier difference map, and in addition a potassium cation was found sandwiched between two aryl rings belonging to two different ligands, L. This suggests the formula K[LNi(μ-H)$_2$NiL],

---

(19) Sheldrick, G. M. *SADABS*; Georg-August-Universität: Göttingen, Germany, 2004.

(20) Spek, A. L. *J. Appl. Crystallogr.* **2003**, *36*, 7–13.

(21) Sheldrick, G. M. *SHELXS-97*; Georg-August-Universität: Göttingen, Germany, 1997.

(22) Sheldrick, G. M. *SHELXL-97*; Georg-August-Universität: Göttingen, Germany, 1997.

(23) (a) O'Connor C. J. *Prog. Inorg. Chem.* **1982**, *29*. (b) Weast, R. C., Astle, M. J., Eds. *CRC Handbook of Chemistry and Physics*; CRC Press Inc.: Boca Raton, FL, 1979.

(24) Bill, E. *julX*: Max-Planck Institut für Bioanorganische Chemie: Mülheim/Ruhr, 2008.

(25) Frisch, M. J.; et al. *Gaussian 03*, Revision D.01; Gaussian, Inc.: Wallingford, CT, 2004.

(26) (a) Becke, A. D. *Phys. Rev. A* **1988**, *38*, 3098–3100. (b) Lee, C.; Yang, W.; Parr, R. G. *Phys. Rev. B* **1988**, *37*, 785–789. (c) Becke, A. D. *J. Chem. Phys.* **1993**, *98*, 5648–5652.

(27) (a) Ditchfield, R.; Hehre, W. J.; Pople, J. A. *J. Chem. Phys.* **1971**, *54*, 724–728. (b) Binning, R. C., Jr.; Curtiss, L. A. *J. Comput. Chem.* **1990**, *11*, 1206–1216. (c) Rassolov, V. A.; Ratner, M. A.; Pople, J. A.; Redfern, P. C.; Curtiss, L. A. *J. Comput. Chem.* **2001**, *22*, 976–984.

(28) Neese, F. *ORCA: An ab Initio, Density Functional and Semiempirical Program Package*, Version 2.7; University of Bonn: Bonn, Germany, 2009.

(29) (a) Carpenter, J. E.; Weinhold, F. *J. Mol. Struct. (THEOCHEM)* **1988**, *169*, 41–62. (b) Reed, A. E.; Curtiss, L. A.; Weinhold, F. *Chem. Rev.* **1988**, *88*, 899–926.

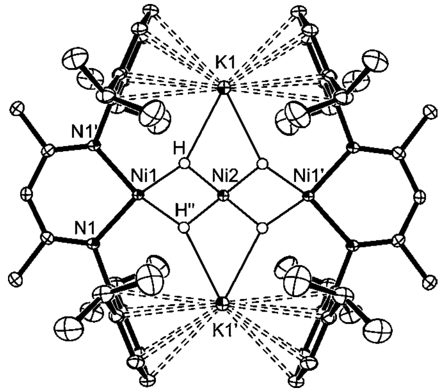

Figure 2. Molecular structure of **4** using 50% thermal ellipsoids. Solvent molecules and carbon−hydrogen atoms are omitted for clarity. Selected bond lengths (Å) and angles (°): N1−Ni1 1.9151(11), Ni1−Ni2 2.4611(3), Ni2−K1 3.1202(5), Ni1−H 1.62(3), Ni2−H˝ 1.47(3), K1−H 2.47(3); Ni1−H′−Ni2 105.0(15), N1′−Ni1-N1 95.58(7), Ni1−Ni2−Ni1’ 180.0, K1−Ni2−K1´ 180.0, Ni1−Ni2−K1 90.0.

3, differing from the *constitution* of **1** in a potassium atom. The *structure* of the LNi(μ-H)$_2$NiL unit can be formally derived from the one found for **1**[12] by a bending across the H−H axis. Interestingly this leads to one metal center coordinated in a square-planar fashion with short Ni−H distances of 1.49(5) and 1.43(5) Å, while the second nickel atom shows a distorted tetrahedral coordination environment with significantly longer Ni−H interactions of 1.61(5) and 1.64(5) Å, respectively. This structural situation suggests the presence of a low-spin d^8-Ni^{II} center ($S' = 0$) and a d^9-Ni^{I} center ($S = 1/2$) with localized valences. Consistently, a SQUID measurement showed an $S = 1/2$ behavior in the entire temperature range investigated (see Supporting Information). The conclusion is further supported by the large anisotropy of the EPR spectrum of **3** in frozen hexane solutions, showing g values of 2.535, 2.196 and 2.056, respectively, and also by DFT calculations (B3LYP/6-31G**): The structure obtained from geometry optimization for **3** was in excellent agreement with the experimental one confirming the thermodynamic preference of the asymmetric hydride distribution between the Ni centers, and indeed a doublet ground state was found in consistency with the suggested electronic structure. In addition an EPR spectrum of the deuterated compound **3-D$_2$** was recorded. The spectra of deuterated and nondeuterated samples deviate, but not in a manner that could be traced to different hyperfine coupling of hydride and deuteride ligands (see Supporting Information).

Naturally, these findings suggested experiments directed toward a further reduction of **3**, and **1** was therefore treated with two equivalents of KC$_8$. This led to a dark purple solution, from which dark purple colored crystals could be isolated (reproducibly and in good yields). These were investigated by XRD, and the result is shown in Figure 2. Two LNi moieties are linked via a NiH$_4$ unit (whose H atoms could be located in the Fourier difference map (residual electron density: 0.6 electrons, see Supporting Information)) such that a planar LNi(μ-H)$_2$Ni(μ-H)$_2$NiL assembly results with short Ni2−H bonds (1.47(3) Å) and longer distances between the hydride ligands and the Ni1 and Ni1’ atoms (1.62(3) Å). Additionally two K$^+$ ions are located within this plane electrostatically interacting with the aryl rings of L, which leads to the formula K$_2$[LNi(μ-H)$_2$Ni(μ-H)$_2$NiL], **4**.

To our knowledge **4** represents the first structurally characterized molecular compound with three nickel atoms bridged by hydride ligands and also the first one containing a [NiH$_4$]$^{2-}$ moiety: In the literature several compounds are known where - similar to the central nickel ion in **4** - a transition metal center gets exclusively coordinated by hydride ligands. Common examples are polyhydride cluster compounds with second and third row transition metal ions,[30] borohydride adduct complexes of early transition metal ions[31] as well as salt-like compounds with transition metal hydride anions like [ReH$_9$]$^{2-}$ or [FeH$_6$]$^{2-}$.[32,33] Moreover several heteronuclear compounds have been described, wherein monovalent group 11 ions are coordinated in a square-planar fashion by terminal hydride ligands of stable metal hydride complex units.[34] However, **4** represents the first coordination compound containing this structural motif with nickel as the central metal atom that has been characterized by means of X-ray crystallography. The Ni−Ni distances of 2.4611(3) Å are significantly longer than those reported for a unit composed of three Ni^{II} centers held together by di-2,2′-pyridylamide ligands after single-electron oxidation (Ni−Ni: 2.283(1) Å). In the latter compound the ligand framework generates square-planar coordination spheres such that the planes are oriented parallel to each other, and hence metal−metal bonding interactions become possible, which are clearly absent in **4**, where the squares share edges.[35]

The ^{1}H NMR spectrum of **4** dissolved in toluene-d_8 showed a characteristic set of sharp signals for the β-diketiminato unit L, but apart from that no further signals were observed in the region where typically hydride ligands of diamagnetic nickel hydrides resonate (from −6 to −26 ppm).[3−6,36] However, a very broad signal with an integral equivalent to four nuclei could be made out at around −37 ppm at 20 °C, which sharpened and shifted to lower field upon cooling ($\delta = -29.76$ ppm at −60 °C, see Figure 3a). This signal can be assigned to hydride nuclei, which are subjected to temperature-dependent paramagnetic interaction, which means that **4** represents a spin-coupled system with a diamagnetic ground state ($S_{\text{total}} = 0$) and a thermally accessible excited triplet state. The singlet ground state can be rationalized when formally two equivalents of LK are subtracted from **4**. The remaining Ni$_3$H$_4$ entity can be described by two paramagnetic Ni^I ($S_{\text{Ni}} = 1/2$) and a central Ni^{II} center that due to the strong square-planar coordination by four hydride ligands is diamagnetic (→ [Ni^{II}H$_4$]$^{2-}$). The magnetic orbitals of the terminal Ni^I ions in planar coordination, (x^2−y^2), are non-orthogonal and therefore antiferromagnetically coupled,[37]

---

(30) (a) Bachechi, F. *J. Organomet. Chem.* **1994**, *474*, 191–197. (b) Bachechi, F.; Bianchini, C.; Meli, A. *Inorg. Chim. Acta* **1993**, *213*, 269–277. (c) Brayshaw, S. K.; Green, J. C.; Edge, R.; McInnes, E. J.; Raithby, P. R.; Warren, J. E.; Weller, A. S. *Angew. Chem., Int. Ed.* **2007**, *46*, 7844–7848. (d) Ciani, G.; Moret, M.; Sironi, A.; Antognazza, P.; Beringhelli, T.; D’Alfonso, G.; Della Pergola, R.; Minoja, A. *J. Chem. Soc., Chem. Commun.* **1991**, 1255–1257. (e) Ginsberg, A. P.; Abrahams, S. C.; Marsh, P.; Ataka, A.; Sprinkle, C. R. *J. Chem. Soc., Chem. Commun.* **1984**, 1321–1323. (f) Lau, J. P.-K.; Wong, W.-T. *Dalton Trans.* **2005**, 2579–2587. (g) Li, X.; Baldamus, J.; Nishiura, M.; Tardif, O.; Hou, Z. *Angew. Chem., Int. Ed.* **2006**, *45*, 8184–8188.

(31) (a) Bansemer, R. L.; Huffman, J. C.; Caulton, K. G. *J. Am. Chem. Soc.* **1983**, *105*, 6163–6164. (b) Bird, P. H.; Churchill, M. R. *Chem. Commun.* **1967**, 403. (c) Broach, R. W.; Chuang, I. S.; Marks, T. J.; Williams, J. M. *Inorg. Chem.* **1983**, *22*, 1081–1084. (d) Ding, E.; Du, B.; Liu, F.-C.; Liu, S.; Meyers, E. A.; Shore, S. G. *Inorg. Chem.* **2005**, *44*, 4871–4878. (e) Ding, E.; Du, B.; Meyers, E. A.; Shore, S. G.; Yousufuddin, M.; Bau, R.; McIntyre, G. J. *Inorg. Chem.* **2005**, *44*, 2459–2464. (f) Ding, E.; Du, B.; Shore, S. G. *J. Organomet. Chem.* **2007**, *692*, 2148–2152. (g) Gozum, J. E.; Girolami, G. S. *J. Am. Chem. Soc.* **1991**, *113*, 3829–3837. (h) Shimoi, M.; Katoh, K.; Tobita, H.; Ogino, H. *Inorg. Chem.* **1990**, *29*, 814–817. (i) Shinomoto, R.; Gamp, E.; Edelstein, N. M.; Templeton, D. H.; Zalkin, A. *Inorg. Chem.* **1983**, *22*, 2351–2355. (j) Welling, U.; Paetzold, P.; Englert, U. *Inorg. Chim. Acta* **1995**, *231*, 175–180.

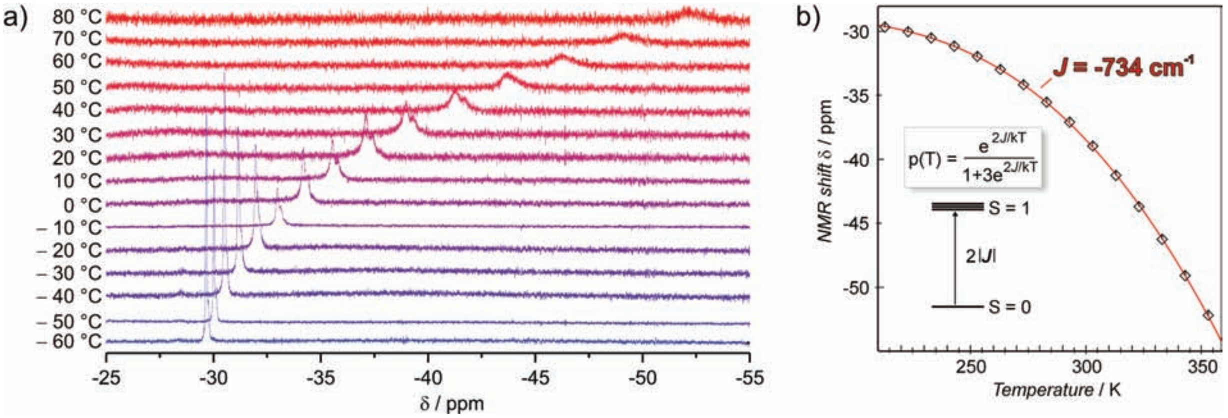

Figure 3. (a) The hydride region of ^{1}H NMR spectra recorded for $K_2[(LNi)_2Ni(\mu\text{-}H)_4]$, **4**, (dissolved in toluene-d_8) showing the temperature dependence of the hydride signal shift and line width and (b) simulation by using the Boltzmann function for a singlet−triplet system with exchange splitting of $2|J|$ (as obtained for a Heisenberg−Dirac−VanVleck Hamiltonian in the notation $H_{\mathrm{HDVV}} = -2JS_1\cdot S_2$). The onset of thermal population of the triplet above ∼200 K causes a temperature-dependent magnetization $m(T)$ of the Ni(I)−Ni(II)−Ni(I) center, which is proportional to the *population difference* of m_s levels for $S = 1$. Assuming fast electronic spin relaxation, the hydride nuclei experience an average field proportional to $m(T)$, and the NMR lines therefore exhibit temperature-dependent shifts according to $\delta(T) = \delta_0 + \delta_p\cdot m(T)$, where δ_0 is the line position for the sample in the diamagnetic ground state ($S = 0$), δ_p is a coefficient for the paramagnetic shift. The magnetization can be approximated by the expression $m(T) = \mathrm{const}\cdot p(T)/T$, where $p(T)$ is the Boltzmann population of the triplet, $p(T) = e^{2J/kT}/\{1 + 3e^{2J/kT}\}$. Moreover, the factor $1/T$ corresponds to the usual Curie-behavior of the magnetization, as it would be observed in case of a triplet ground state. This simple approach for $m(T)$ is valid here, because the Zeeman splitting Δ_Z of the triplet is very small ($\Delta_Z \ll kT$). The corresponding expression for $\delta(T)$ yields an excellent fit to the experimental data with the value $J = -734$ cm^{-1} for the exchange coupling constant (red line in Figure 3b).

mediated by superexchange through the diamagnetic central $[Ni^{II}H_4]^{2-}$ unit.

The singlet−triplet gap of **4** could be determined from the temperature dependence of the hydride NMR line positions. Assuming fast spin relaxation between the singlet and the triplet magnetic substates the protons experience an average electronic magnetization $m(T) \propto p(T)/T$, where $p(T)$ is the Boltzmann population of the triplet. Fitting of the appropriate Boltzmann function to the experimental data (Figure 3b) revealed an exchange coupling constant of $J = -734$ cm^{-1} (for $H = -2JS_1\cdot S_2$), meaning that spin coupling is very strong and that the triplet state of **4** lies 17.6 kJmol^{-1} above the singlet state. We note in passing that such a large singlet triplet splitting (corresponding to a thermal energy of $E/k = 2112$ K) can be hardly detected by usual static magnetic susceptibility measurements (SQUID), because the thermal population of the triplet at 300 K is only about 0.08%, and the induced effective moment with 1 T applied field corresponds to about 0.1 μ_B, which can be hardly discriminated from background signals due to traces of impurity and temperature-independent paramagnetism (TIP).

4 is not only remarkable with respect to its electronic properties or its structure but also chemically: Interestingly, on storage of NMR samples of **4** dissolved in benzene-d_6 or toluene-d_8 at room temperature it was found to undergo H/D exchange with the solvent. The broad signal of the hydride ligands converts into a set of several signals (corresponding to species with varying degrees of deuteration), and the integral decreases (Figure 4a); a complete H/D exchange was accomplished within 16 h at 60 °C. Subsequently, a ^{2}H NMR spectrum recorded for a benzene solution at room temperature (Figure 4b) indeed showed a signal at −37.21 ppm (Ni_3D_4), being approximately 7 times sharper than the hydride signal in the ^{1}H NMR spectrum (as expected, due to a smaller gyromagnetic constant of ^{2}H relative to that of ^{1}H, compare ref 38). An additional smaller signal at −37.53 ppm points to the presence of a small percentage of ^{1}H, presumably due to D/H exchange after redissolution of the fully deuterated sample in benzene for the ^{2}H NMR measurement. In addition, two signals at 1.83 ppm and 1.12 ppm were observed, indicating incorporation of D also into the methyl residues of the ^{i}propyl substituents of the ligand (see Figure 4). Similar reactivities had been found before for $LPtMe_3$,[39] and for the iridium hydride $LIrH_4$,[40] but only the latter also showed selective deuterium incorporation into the methyl residues. This was explained by reversible reductive elimination of H_2 and oxidative addition of C−D units or C−H units from the ^{i}propyl residue, whose methyl groups

---

(32) (a) Abrahams, S. C.; Ginsberg, A. P.; Knox, K. *Inorg. Chem.* **1964**, *3*, 558–567. (b) Knox, K.; Ginsberg, A. P. *Inorg. Chem.* **1964**, *3*, 555–558.

(33) Bau, R.; Ho, D. M.; Gibbins, S. G. *J. Am. Chem. Soc.* **1981**, *103*, 4960–4962.

(34) (a) Rhodes, L. F.; Huffman, J. C.; Caulton, K. G. *J. Am. Chem. Soc.* **1983**, *105*, 5137–5138. (b) Rhodes, L. F.; Huffman, J. C.; Caulton, K. G. *J. Am. Chem. Soc.* **1984**, *106*, 6874–6876. (c) Rhodes, L. F.; Huffman, J. C.; Caulton, K. G. *Inorg. Chim. Acta* **1992**, *198*−*200*, 639–649. (d) Antinolo, A.; Carrillo, F.; Chaudret, B.; Fajardo, M.; Fernandez-Baeza, J.; Lanfranchi, M.; Limbach, H.-H.; Maurer, M.; Otero, A.; Pellinghelli, M. A. *Inorg. Chem.* **1994**, *33*, 5163–5164. (e) Luo, S.; Burns, C. J.; Kubas, G. J.; Bryan, J. C.; Crabtree, R. H. *J. Cluster Sci.* **2000**, *11*, 189–216. (f) Brunner, H.; Mijolovic, D.; Wrackmeyer, B.; Nuber, B. *J. Organomet. Chem.* **1999**, *579*, 298–303.

(35) Berry, J. F.; Cotton, F. A.; Daniels, L. M.; Murillo, C. A. *J. Am. Chem. Soc.* **2002**, *124*, 3212–3213.

(36) (a) Vicic, D. A.; Jones, W. D. *J. Am. Chem. Soc.* **1997**, *119*, 10855–10856. (b) Bach, I.; Goddard, R.; Kopiske, C.; Seevogel, K.; Porschke, K.-R. *Organometallics* **1999**, *18*, 10–20. (c) Miedaner, A.; DuBois, D. L.; Curtis, C. J.; Haltiwanger, R. C. *Organometallics* **1993**, *12*, 299–303. (d) Tenorio, M. J.; Puerta, M. C.; Valerga, P. *J. Chem. Soc., Dalton Trans.* **1996**, 1305–1308. (e) Seligson, A. L.; Cowan, R. L.; Trogler, W. C. *Inorg. Chem.* **1991**, *30*, 3371–3381. (f) Abernethy, C. D.; Baker, R. J.; Cole, M. L.; Davies, A. J.; Jones, C. *Transition Met. Chem.* **2003**, *28*, 296–299. (g) Aresta, M.; Quaranta, E.; Dibenedetto, A.; Giannoccaro, P.; Tommasi, I.; Lanfranchi, M.; Tiripicchio, A. *Organometallics* **1997**, *16*, 834–841. (h) He, T.; Tsvetkov, N. P.; Andino, J. G.; Gao, X.; Fullmer, B. C.; Caulton, K. G. *J. Am. Chem. Soc.* **2010**, *132*, 910–911.

(37) Kahn, O. *Molecular Magnetism*; VCH: New York, 1993.

(38) Lanci, M. P.; Smirnov, V. V.; Cramer, C. J.; Gauchenova, E. V.; Sundermeyer, J.; Roth, J. P. *J. Am. Chem. Soc.* **2007**, *129*, 14697–14709.

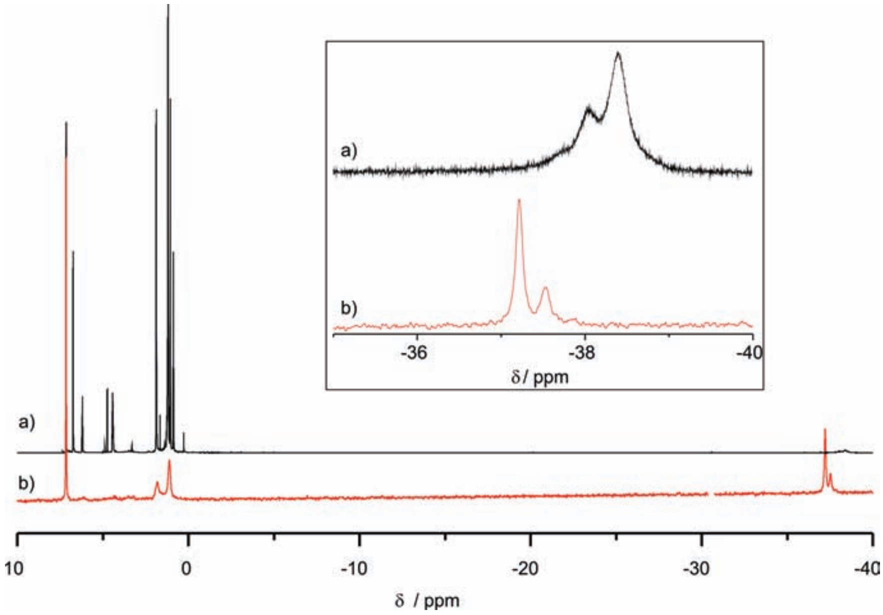

Figure 4. (a) ^{1}H NMR spectrum of $K_2[(LNi)_2Ni(\mu\text{-}H)_4]$, **4**, after storage for one hour in benzene-d_6; the presence of several species with a different degree of deuteration in the hydride positions already becomes obvious; (b) ^{2}H NMR spectrum of the same sample as in a) after heating the mixture for 16 h to 60 °C in benzene-d_6; all hydride signals had vanished in the ^{1}H NMR spectrum, suggesting complete H/D exchange. Subsequently, the solvent was changed to benzene, and the ^{2}H NMR spectrum was recorded. The presence of several deuteride signals indicates that to a small extent D/H exchange with C_6H_6 had occurred already. The different line positions for the hydride/deuteride signals in (a) and (b) are due to isotope effects on the chemical shift which can have various reasons;[48] slightly different temperatures cannot be excluded.

are more readily accessible than the ^{i}propyl methine position. Typically, the oxidative addition of C−H bonds[41] requires electron-rich, low-valent complexes of the second and third row 'late' transition metals such as Re,[42] Ru,[43] Rh,[44] Ir,[45] and Pt,[46] whereas the C−H activation with compounds of the first row element nickel is less common.[47] For **4** we found that the presence of H_2 slows down the H−D exchange with the solvent, which points to an equilibrium involving free H_2 (or a free coordination site that is blocked by H_2). Moreover, when solutions of **4-D$_4$** in benzene-d_6 (generated *in situ*) were exposed to an atmosphere of dihydrogen, the hydride signals reappeared in the ^{1}H NMR spectrum. Consistently, we found that performing the synthesis of **4** in an atmosphere of D_2 as the only source of deuterium leads to a product, whose ^{2}H NMR spectrum is identical to that shown in Figure 4b.

It is difficult to explain the formation of **4**. Given that **1** is reduced to **3** by one equivalent of KC_8, it is reasonable to assume that a second equivalent first of all leads to the nickel(I) hydride dimer $K_2[LNi(\mu\text{-}H)_2NiL]$. Apparently, this highly reduced hydride is unstable and triggers a series of events leading to the extrusion of Ni from a second molecule (or from an unreacted molecule of **3**). NMR spectroscopically the formation of LK was proven (29% yield based on the amount of **1** and 88% of the theoretical yield). Possibly H_2 is intermediately eliminated to give Ni^0 species, to which then H_2 readds; the sensitivity of negatively charged reduced metal hydride entities toward reductive H_2 elimination was shown recently by Holland and co-workers for the case of a similar reduced cobalt hydride compound.[16] As we have reported recently, β-diketiminato nickel(I) complexes with very weak ligation react immediately with toluene to yield the toluene-bridged compound **2**.[14] The fact that, after performing the synthesis of **4** in benzene as the solvent, no analogous benzene complex $[LNi(\mu\text{-}\eta^3\text{:}\eta^3\text{-}C_6H_6)NiL]$ could be detected excludes such simple LNi^I intermediates in the present reaction. Remarkably, the crystalline yield based on the required 2 **1** → **4** stoichiometry amounts to 48%; that is, despite its complexity the reaction is remarkably selective.

To investigate the redox properties of **4** it was treated with various reagents. TlOTf turned out to act as a single-electron oxidant producing $K[LNi(\mu\text{-}H)_2Ni(\mu\text{-}H)_2NiL]$, **5**, (see Scheme 1) with concomitant formation of Tl^0 and KOTf. Crystals of **5** could be grown by evaporation of the solvent from diethyl ether solutions, and a single-crystal X-ray diffraction analysis (see Figure 5) revealed a molecular structure very similar to the one found for **4** with the difference that one of the two K$^+$ ions is missing (in addition to the electron). Clearly this reduces the

---

(39) Fekl, U.; Goldberg, K. I. *J. Am. Chem. Soc.* **2002**, *124*, 6804–6805.

(40) Bernskoetter, W. H.; Lobkovsky, E.; Chirik, P. J. *Chem. Commun.* **2004**, 764–765.

(41) (a) Crabtree, R. H. *Chem. Rev.* **1995**, *95*, 987–1007. (b) Labinger, J. A.; Bercaw, J. E. *Nature* **2002**, *417*, 507–514. (c) Stahl, S. S.; Labinger, J. A.; Bercaw, J. E. *Angew. Chem., Int. Ed.* **1998**, *37*, 2180–2192.

(42) Takaya, H.; Ito, M.; Murahashi, S.-I. *J. Am. Chem. Soc.* **2009**, *131*, 10824–10825.

(43) Ingleson, M. J.; Yang, X.; Pink, M.; Caulton, K. G. *J. Am. Chem. Soc.* **2005**, *127*, 10846–10847.

(44) (a) Chen, H.; Schlecht, S.; Semple, T. C.; Hartwig, J. F. *Science* **2000**, *287*, 1995–1997. (b) Dorta, R.; Stevens, E. D.; Nolan, S. P. *J. Am. Chem. Soc.* **2004**, *126*, 5054–5055. (c) Jones, W. D. *Inorg. Chem.* **2005**, *44*, 4475–4484. (d) Rybtchinski, B.; Cohen, R.; Ben-David, Y.; Martin, J. M. L.; Milstein, D. *J. Am. Chem. Soc.* **2003**, *125*, 11041–11050. (e) Maegawa, T.; Fujiwara, Y.; Inagaki, Y.; Esaki, H.; Monguchi, Y.; Sajiki, H. *Angew. Chem., Int. Ed.* **2008**, *47*, 5394–5397. (f) Verat, A. Y.; Pink, M.; Fan, H.; Tomaszewski, J.; Caulton, K. G. *Organometallics* **2008**, *27*, 166–168.

(45) (a) Arndtsen, B. A.; Bergman, R. G. *Science* **1995**, *270*, 1970–1973. (b) Bhalla, G.; Liu, X. Y.; Oxgaard, J.; Goddard, W. A.; Periana, R. A. *J. Am. Chem. Soc.* **2005**, *127*, 11372–11389. (c) Fan, L.; Parkin, S.; Ozerov, O. V. *J. Am. Chem. Soc.* **2005**, *127*, 16772–16773. (d) Hoyano, J. K.; Graham, W. A. G. *J. Am. Chem. Soc.* **1982**, *104*, 3723–3725. (e) Janowicz, A. H.; Bergman, R. G. *J. Am. Chem. Soc.* **1982**, *104*, 352–354. (f) Kanzelberger, M.; Singh, B.; Czerw, M.; Krogh-Jespersen, K.; Goldman, A. S. *J. Am. Chem. Soc.* **2000**, *122*, 11017–11018. (g) Haenel, M. W.; Oevers, S.; Angermund, K.; Kaska, W. C.; Fan, H.-J.; Hall, M. B. *Angew. Chem., Int. Ed.* **2001**, *40*, 3596–3600.

Scheme 1. Synthesis of **3**, **4**, **5**, and **6**, L = $[HC(CMeNC_6H_3(iPr)_2)_2]^-$

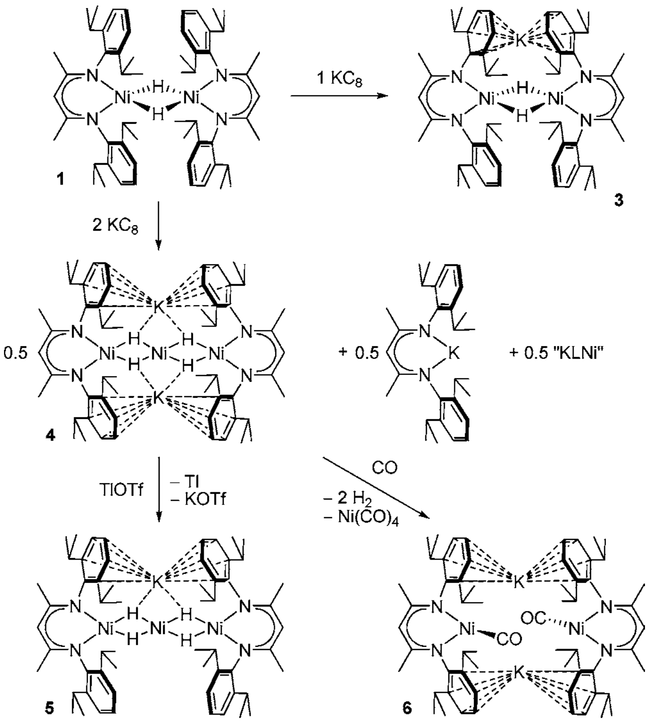

electrostatic interaction of the two LNi fragments, but nevertheless the Ni−Ni-distances decrease to 2.40775(10) and 2.38998(13) Å, simply because of the reduction of the Ni−H distances on going from Ni^I to Ni^{II}. As a result, the whole molecule is slightly distorted as compared to **4**. The Ni−Ni−Ni angle of 176.544(2)° deviates from linearity, and the dihedral angle between the ligand backbones amounts to 9.056(4)°. The removal of one electron from the diamagnetic Ni_3H_4 core naturally results in a paramagnetic compound, and indeed magnetic measurements on **5** in the solid state as well as X-band EPR measurements on frozen hexane solution of **5** at 77 K confirmed the presence of a paramagnetic species with an $S = 1/2$ ground state (see Supporting Information and Figure 6). The EPR spectrum could be simulated reasonably well by adopting a set of rhombic g values (2.513, 2.239, 2.082) and hyperfine interaction with the four hydrogen nuclei (with coupling constants $A_{xx} = 1.7$, $A_{yy} = 2.4$, $A_{zz} = 1.7$ mT), which yet again confirms the presence of four hydride ligands in the starting material **4** (see Figure 6). The hyperfine splitting for the isotopologue **5-D$_4$** was not resolved due to the smaller hyperfine coupling constant for deuterium (see Supporting Information).

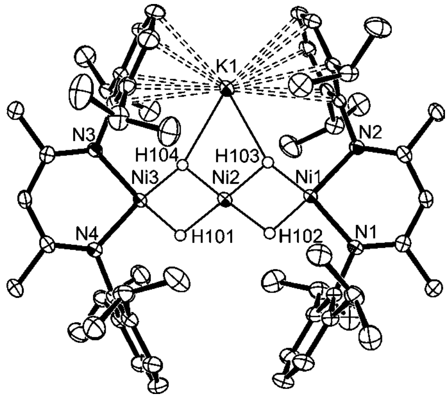

Figure 5. Molecular structure of **5** using 50% thermal ellipsoids. Solvent molecules and carbon−hydrogen atoms are omitted for clarity. Selected bond lengths (Å) and angles (deg): Ni1−H102 1.514(3), Ni1−H103 1.512(3), Ni2−H102 1.561(3), Ni2−H103 1.609(3), Ni1−Ni2 2.40775(10), Ni2−Ni3 2.38998(13), Ni1−N1 1.88468(19), Ni1−N2 1.9039(2), K1−H103 2.517(3), K1−H104 2.521(3); Ni1−Ni2−Ni3 176.544(2), H101−Ni3−H104 77.73(16), N3−Ni3−N4 95.546(9), H104−Ni3−N3 93.48(12), H104−Ni3−N4 170.96(12), H101−Ni3−N4 93.27(10), H101−Ni3−N3 170.79(10), H104−Ni2−H103 103.23(15), H101−Ni2−H102 109.42(15), H104−Ni2−H103 103.23(15), H101−Ni2−H102 109.42(15).

As we had found[12] that addition of neutral donors (such as nitriles) to the LNiH dimer **1** leads to reductive elimination of H_2 with concomitant formation of LNi^I complexes (see above), **4** was also investigated in this respect. Formal elimination of two equivalents of H_2 would lead to three Ni^0 centers, and it seemed interesting to see how such a system behaves. Dissolution of **4** in acetonitrile caused decomposition to untractable products, which already indicated the sensitivity of **4** toward donor ligands. Treatment with CO gas indeed led to the release of H_2 (as observed by ^1H NMR spectroscopy, see Supporting Information), and remarkably at the same time the central Ni atom was extracted in the form of $Ni(CO)_4$ as detected by ^{13}C NMR spectroscopy, while the coordination spheres of the remaining Ni^0 centers were saturated by CO ligands. This resulted in the complex $K_2[LNi(CO)]_2$, **6**, (see Scheme 1) whose molecular structure is shown in Figure 7. Two $LNi^0(CO)$ units with trigonal planar coordinated Ni centers are held together by two K^+ ions. As the two CO ligands are repelling each other, these two units cannot be oriented within one plane, and the Ni centers are situated ~0.28 Å above the plane defined by the diketiminato moiety. K−O distances not going below 2.974(3) Å appear too long to suggest discrete K−O interactions. As expected, **6** is diamagnetic, and its ν(CO) modes absorb at far lower wave numbers (1772, 1754 cm^{-1}) than ν(CO) of the Ni^I complex [LNi(CO)] (2022 cm^{-1}).[49]

Conclusions

In summary we have shown that the nickel(II)hydride dimer, $[LNi(\mu\text{-}H)]_2$, **1**, can accept one electron to give a mixed-valent Ni^INi^{II} hydride compound with localized spins.

---

(46) (a) Holtcamp, M. W.; Labinger, J. A.; Bercaw, J. E. *J. Am. Chem. Soc.* **1997**, *119*, 848–849. (b) Wick, D. D.; Goldberg, K. I. *J. Am. Chem. Soc.* **1997**, *119*, 10235–10236. (c) Reinartz, S.; White, P. S.; Brookhart, M.; Templeton, J. L. *J. Am. Chem. Soc.* **2001**, *123*, 12724–12725. (d) Kloek, S. M.; Goldberg, K. I. *J. Am. Chem. Soc.* **2007**, *129*, 3460–3461. (e) Thomas, J. C.; Peters, J. C. *J. Am. Chem. Soc.* **2003**, *125*, 8870–8888. (f) Driver, T. G.; Williams, T. J.; Labinger, J. A.; Bercaw, J. E. *Organometallics* **2007**, *26*, 294–301. (g) Konze, W. V.; Scott, B. L.; Kubas, G. J. *J. Am. Chem. Soc.* **2002**, *124*, 12550–12556. (h) Lersch, M.; Tilset, M. *Chem. Rev.* **2005**, *105*, 2471–2526.

(47) (a) Niu, J.-L.; Chen, Q.-T.; Hao, X.-Q.; Zhao, Q.-X.; Gong, J.-F.; Song, M.-P. *Organometallics* **2010**, *29*, 2148–2156. (b) Liang, L.-C.; Chien, P.-S.; Huang, Y.-L. *J. Am. Chem. Soc.* **2006**, *128*, 15562–15563. (c) Brunkan, N. M.; Brestensky, D. M.; Jones, W. D. *J. Am. Chem. Soc.* **2004**, *126*, 3627–3641. (d) Keen, A. L.; Johnson, S. A. *J. Am. Chem. Soc.* **2006**, *128*, 1806–1807. (e) van der Boom, M. E.; Liou, S.-Y.; Shimon, L. J. W.; Ben-David, Y.; Milstein, D. *Inorg. Chim. Acta* **2004**, *357*, 4015–4023. (f) Davis, S. C.; Severson, S. J.; Klabunde, K. J. *J. Am. Chem. Soc.* **1981**, *103*, 3024–3029. (g) Castonguay, A.; Sui-Seng, C.; Zargarian, D.; Beauchamp, A. L. *Organometallics* **2006**, *25*, 602–608.

(48) For isotope effects on the chemical shift ("isotopic shifts") due to different H/D isomers compare for instance: Göttker-Schnetmann, I.; Heinekey, D. M.; Brookhart, M. *J. Am. Chem. Soc.* **2006**, *128*, 17114−17119.

(49) Eckert, N. A.; Dinescu, A.; Cundari, T. R.; Holland, P. L. *Inorg. Chem.* **2005**, *44*, 7702–7704.

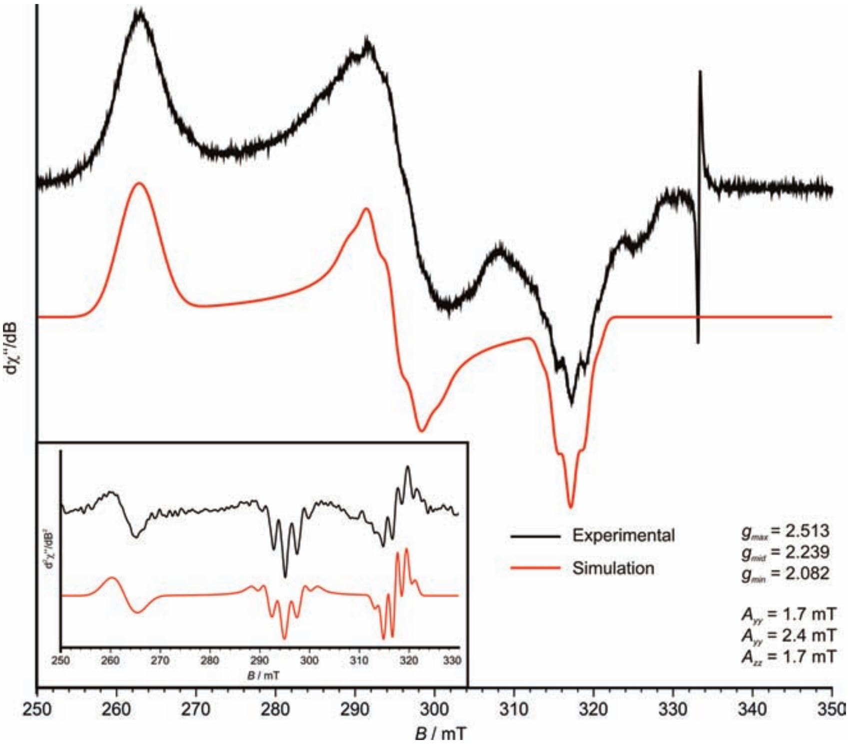

Figure 6. X-band EPR spectrum of $K[(LNi)_2Ni(\mu\text{-}H)_4]$, **5**, in hexane at 77 K (microwave frequency 9.246 GHz, power 2 mW, modulation 0.125 mT/100 kHz). The red line is a powder simulation with *g* and *A* values as indicated. The inset shows the second-derivative spectrum and simulation.

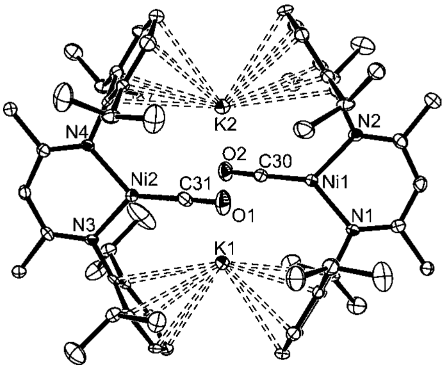

Figure 7. Molecular structure of **6** using 50% thermal ellipsoids. Solvent molecules and hydrogen atoms are omitted for clarity. Selected bond lengths (Å) and angles (deg): N1−Ni1 1.918(3), N2−Ni1 1.922(3), N3−Ni2 1.921(3), N4−Ni2 1.923(3), Ni1−C30 1.665(4), Ni2−C31 1.664(4), C30−O2 1.191(5), C31−O1 1.183(5), K1−C31 2.916(4), K1−O1 2.995(4), K1−C30 2.940(4), K1−O2 3.001(3); N1−Ni1−N2 93.86(14), N1−Ni1−C30 134.93(17), N2−Ni1−C30 130.72(18), Ni1−C30−O2 178.7(4), N3−Ni2−N4 95.53(14), N3−Ni2−C31 133.18(18), N4−Ni2−C31 130.63(18), Ni2−C31−O1 178.1(4).

Further reduction, however, triggers a complicated reaction sequence that reproducibly and in good yields leads to the complex $K_2[(LNi)_2Ni(\mu\text{-}H)_4]$, **4**, with an unprecedented Ni_3H_4 core: **4** is the first structurally characterized complex that contains a nickel center homoleptically coordinated by hydride ligands. **4** has a singlet ground state but a low-lying triplet state that can be thermally populated and thus leads to a peculiar shift of the hydride signal in the ^1H NMR spectrum. It is possible to singly oxidize **4** as illustrated by its reaction with TlOTf, and its sensitivity with respect to the elimination of H_2 becomes obvious, noting that treatment with CO leads to $K_2[LNi(CO)]_2$, **6**, H_2, and $Ni(CO)_4$. In contact with deuterated solvents such as toluene-d_8 or benzene-d_6 **4** exchanges its hydride ligands against deuteride, and H/D exchanges are also observed in an H_2/D_2 atmosphere. Future research will now focus on the further elucidation of the detailed mechanism of these H/D exchange reactions and on the nature of the interaction of H_2 and hydrocarbons with **4** or a reactive species generated from it.

Altogether the results show that nickel hydrides can offer a versatile redox chemistry leading to remarkable structural and electronic situations as well as to interesting reactivities, as exploited by the [NiFe]-hydrogenases.

Acknowledgment. We are grateful to the Cluster of Excellence “Unifying Concepts in Catalysis” funded by the *Deutsche Forschungsgemeinschaft* (DFG), the Fonds der Chemischen Industrie, and the Humboldt-Universität zu Berlin for financial support. We thank Ulli Englert for crystallographic support and Michael Teltewskoi for support with ^2H NMR measurements. We also would like to acknowledge valuable discussions with Thomas Braun, Alexander C. Filippou, Frank Neese and Joachim Sauer.

Supporting Information Available: Complete ref 25, NMR spectra of **4** and **6**, EPR-spectra of **3**, **3-D$_2$**, and **5-D$_4$**, details on magnetic measurements for **3** and **5**, computational details, crystallographic data, and CIF files. This material is available free of charge via the Internet at http://pubs.acs.org.

JA106266V